Journal of Innovative Optical Health Sciences
Vol. 7, No. 3 (2014) 1350059 (7 pages)

DOI: 10.1142/S1793545813500594

World Scientific
www.worldscientific.com

Synthesis of biocompatible near infrared fluorescence Ag_2S quantum dot and its application in bioimaging

Xin Zhang, Yueqing Gu* and Haiyan Chen†
Department of Biomedical Engineering
School of Life Science and Technology
China Pharmaceutical University, 24 Tongjia Lane
Gulou District, Nanjing 210009, P. R. China
**guyueqingsubmission@hotmail.com*
†*chenhaiyan@cpu.edu.cn*

Received 31 May 2013
Accepted 15 September 2013
Published 28 November 2013

Near infrared (NIR) emitting quantum dots (QDs) is a promising candidate for biomedical imaging in living tissues. However, the biomedical application of NIR QDs was not satisfactory due to their toxicity. Ag_2S QDs was reported to have negligible toxicity in organisms. Therefore, the appropriate narrow bandgap and low toxicity of Ag_2S QDs facilitated them to be a promising contrast agent for fluorescence imaging. Here, a low toxicity, stable and highly luminescent NIR Ag_2S QDs were prepared by one-step aqueous method using 2-mercaptopropionic acid (MPA) as the coating layers. Emission wavelength of Ag_2S QDs could be tuned between 780 and 950 nm. MTT assay results indicated that there was no significant biotoxicty for Ag_2S QDs. These NIR QDs exhibited excellent biocompatibility in tumor cells. The cellular uptake and localization of Ag_2S QDs was studied using laser confocal scanning microscopy. Ag_2S QDs were effectively internalized by the cells. Therefore, Ag_2S QDs, acting as a novel fluorescence probe, has promising potential in biolabeling, deep tissue imaging, diagnostics and photodynamic therapy.

Keywords: Near infrared fluorescence quantum dot; toxicity; bioimaging.

1. Introduction

Quantum dots (QDs) are widely used for biolabeling and bioimaging because of their distinct advantages in optical properties such as great photostability, high photoluminescence efficiency, size-dependent emission and a sharp emission profile.[1–5] However, QDs that are excited in the UV emit in the visible region are not practical for bio-applications. Firstly, biological constituents, like water, hemoglobin and deoxyhemoglobin absorb and scatter light in the visible region (400–700 nm) and therefore have a quenching effect.[6–8] Secondly, living tissue

(like collagen)[9] has significant auto-fluorescence in the visible region.[10] Thirdly, the penetration depth of visible light is limited.[10,11] Near-infrared (NIR) light solves the auto-fluorescence problem by reducing the fluorescence background, making NIR QDs a promising candidate for biomedical imaging in living tissues.[12–15] Some typical examples of NIRQDs reported in the literature are CdSeTe, CdSeTe/Cd, CdHgTe/CdS, CdTe/CdSe/ZnSe[16–18] and PbS.[9] There are a few NIR QDs that have been used successfully in *in vivo* imaging. Morgan *et al.*[19] used CdMnTe/HgQDs as an angiographic contrast agent. Kim *et al.*[20] demonstrated imaging of sentinel lymph nodes in mice with CdTe/CdSe QDs. Ding *et al.*[21] used CdTe/ZnS QDs in the imaging of a PANC-1 tumor. However, apart from the imaging window consideration, toxicity is another important roadblock in the practical use of QDs, especially for *in vivo* bio-applications. For bioimaging, the QDs emission wavelength should ideally be in the NIR region to improve tissue penetration depth and to reduce background fluorescence.[22–24] Moreover, NIR fluorescent QDs for *in vivo* imaging not only need excellent optical performance, but should also be ultrasmall in size and free of extremely toxic elements, such as Cd, Pb and Hg.[25,26] However, it is still challenging to prepare NIR fluorescent QDs with ultrasmall size and low toxicity for bioimaging applications. A few aqueous synthetic strategies for water-soluble NIR fluorescent Ag_2S QDs have also been reported to avoid a further phase transfer process for bio-application.[27–30] Pang's group[27] made the first attempt to synthesize water-soluble carboxylic acid group terminated Ag_2S QDs with tunable emissions in ethylene glycol by a one-step method, and directly injected the Ag_2S QDs with the emission at 910 nm into the subcutaneous tissue and the abdominal cavity for small animal imaging. However, previous methods for preparing water-soluble Ag_2S QDs still require high temperature, argon gas protection and a nonaqueous solvent.[27,28] Furthermore, previous applications of Ag_2S QDs were also limited only for cell imaging[29] and nontargeted small animal imaging.[27] Therefore, it is of great interest to develop a mild and effective route for preparing functionalized water-soluble NIR fluorescent Ag_2S QDs for targeted tumor imaging *in vivo*.

Herein, a one-step synthesis of 2-mercaptopropionic acid (3-MPA)-coated aqueous Ag_2S NIRQDs was demonstrated, and the bioconjugation of the Ag_2S QDs with a new developed peptide for targeted cancer imaging *in vivo*.[31] 3-MPA-coated Ag_2S QDs are firstly synthesized in aqueous solution via a simple and mild synthetic route at 90°C and N_2 gas protection. The resulting Ag_2S QDs exhibit intense NIR fluorescence, ultrasmall size and low *in vivo* toxicity, which are favorable for bioimaging. 3-MPA not only acts as a stabilizer, but also facilitates post-surface modifications with functional biomolecules. As the peptide plays a role in tumor target and has enormous potential as a diagnostic and prognostic biomarker of the disease status, further bioconjugation of Ag_2S QDs with peptide allows targeted imaging. For potential biological uses, the cytocompatibility of particles was investigated and *in vitro* imaging using MCF-7 cell lines was demonstrated.[32–39]

2. Materials and Experiments

2.1. *Materials*

All reagents were analytical grade or highest purity. Silver nitrate ($AgNO_3$) was purchased from Sigma-Aldrich. Sodium sulfide (Na_2S) was purchased from Alfa-Aesar. 3-Mercaptopropionic acid (3-MPA), acetic acid (CH_3COOH), sodium hydroxide (NaOH), phosphate buffered saline (PBS), dimethyl sulfoxide (DMSO), and 4% paraformaldehyde were purchased from Merck. LDS 798 near-IR laser dye was purchased from Exciton Inc. Milli-Q water (18 mU) was used as the solvent. DMEM medium (with 1.0 g/L glucose, stable L-glutamine, 3.7 g/L $NaHCO_3$ and phenol red, 10% fetal bovine serum and trypsin-EDTA were purchased from Biochrom AG, Germany. 1% penicillin–streptomycin antibiotic solution was purchased from HyClone, USA. Sodium30-[1-(phenylaminocarbonyl)-3,4-tetrazolium]-bis(4-methoxy-6-nitro) benzene sulfonic acid hydrate (MTT) was purchased from Biological Industries, Israel. 96-well plates were purchased from Greiner Bio-One, Germany.

2.2. *Preparation of Ag_2S nanoparticles*

Typically, 3-MPA was dissolved in 75 mL of deoxygenated deionized water. The pH of the solution was adjusted to 7.5 using NaOH and CH_3COOH solutions (2 M). Then $AgNO_3$ (42.5 mg) was added, the pH was readjusted to 7.5 and the solution was brought to the desired temperature (30°C, 50°C or 90°C). About 25 mL of deoxygenated aqueous Na_2S solution was then added slowly to the reaction

mixture under vigorous mechanical stirring at 5000 rpm. During the reaction, samples were taken at different time points to follow the particle growth. The product was stored in the dark at 4°C for further analysis.

2.3. *Characterization methods*

The absorption spectra of Ag_2S QDs were acquired with Lambda 25 UV-Vis spectrophotometer (Perkin Elmer, US). The corresponding fluorescence spectra of the materials were measured at room temperature using a LS 55 Fluorescence Spectrometer (Perkin Elmer, US).

2.4. *Cell culture*

Culturing of human breast cancer cells (MCF-7) was done according to ATCC recommendations. Cells were cultured in DMEM medium with 1.0 g glucose, stable L-glutamine, 3.7 g $NaHCO_3$ and phenol red. Full medium also contained 10% fetal bovine serum and 1% penicillin–streptomycin antibiotic solution. Trypsin-EDTA was used for cell detachment. Cells were incubated at 37°C under 5% CO_2.

2.5. *Evaluation of cytotoxicity*

MTT assay was used for the evaluation of cytotoxicity. About 5000 cells per well in 96-well plates were seeded. Following overnight incubation, after treating the cells with different concentrations (0.02 to l2.5 μM) of Ag_2S QDs, the cells were further maintained at 37°C for 24 h. Each well was replaced and the cells were washed three times with PBS (pH 7.0) before addition of 20 μL of MTT solution (5.0 μg/mL). After incubating another 4 h, the medium containing MTT was carefully removed from each well and DMSO (150 μL) was added to each well to dissolve the purple crystals. The plates were gently shaken for 10 min at room temperature before measuring the absorbance. Spectrophotometric readings were taken at 500 and 650 nm. Absorbance at 650 nm was subtracted from the absorbance at 500 nm which corrects the results for the QD absorbance. All test samples were assayed in quadruplicate and the cell viability was calculated using the following formula: Cell viability = (Mean absorbance of test wells − Mean absorbance of medium control wells)/(Mean absorbance of untreated wells − Mean absorbance of medium control well) × 100%. We also verified the low toxicity of Ag_2S QDs through animal experiment. The mice injected with Ag_2S QDs (1062.5 μg/kg) did not show any abnormal symptoms.

2.6. *Cell imaging*

Cellular uptake and localization of Ag_2S QDs were evaluated using MCF-7 cell. The cells were seeded in laser confocal fluorescence microscope (LCFM) culture dishes with a density of 4×105 cells/well and subsequently incubated at 37°C. When the whole cells reached ∼70–80% confluency, 20 μL of QDs were added into different dishes and then incubated for 2 and 4 h. The cell affinity of the QDs was detected by LCFM (FV1000, Olympus, Japan). The red fluorescence of Ag_2S QDs was captured under 488-nm light excitation. Intracellular uptake of the different probes was determined from the red fluorescence intensity in the region of interest (ROI) using Scion Image software.

3. Results and Discussion

3.1. *Synthesis and characterization of 3-MPA-coated Ag_2S NIR QDs*

3-MPA-coated Ag_2S QDs were prepared in water with slow addition of sulfide to a mixture of 3-MPA and silver salt. The color of the solution turned yellow with the addition of sulfide ion and the resulting colloidal QDs solution had a dark brown color. The Ag_2S QDs exhibit favorable optical properties. The photoluminescence emission peak of the Ag_2S QDs is 800 nm in the NIR region. The quantum yields of synthesized Ag_2S QDs was 37.9 %. The fluorescence spectra show the emission peak centered at 800 nm with an impressive full width at half maximum of 75 nm, indicating a narrow size distribution of the Ag_2S QDs. The UV-vis spectra of the Ag_2S QDs show a feature around 450 nm [see Fig. 1(a)]. The luminescence spectrum of the Ag_2S QDs with emission at 800 nm was distinctly detected via the LS 55 Fluorescence Spectrometer [see Fig. 1(b)]. Emission wavelength of Ag_2S QDs could be tuned between 800 and 830 nm, which was shown in Fig. 1(c).

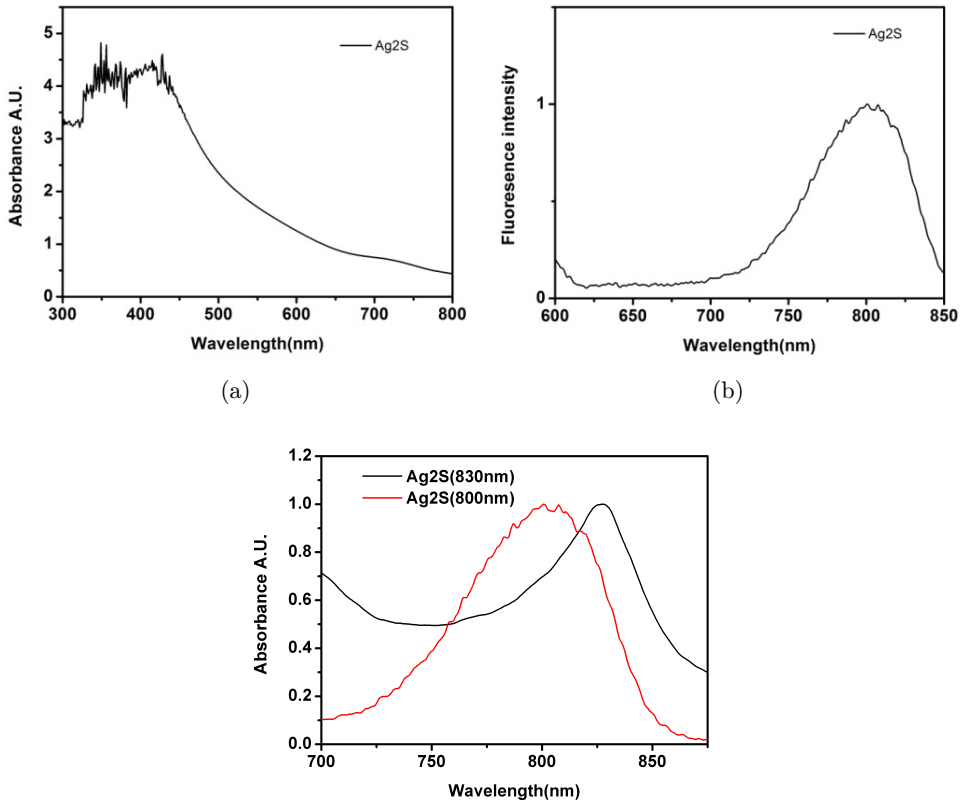

Fig. 1. (a) Absorption spectra of Ag_2S QDs; (b) Fluorescence spectrum of Ag_2S QDs; (c) Fluorescence spectra of the Ag_2S QDs with different emission wavelength.

3.2. *Evaluation of cytotoxicity*

The cytotoxicity of Ag_2S QDs was tested on MCF-7 human breast cancer cells using MTT assay. The Ag_2S QDs did not show significant cytotoxicity at concentrations up to 0.425 mg/mL, with more than 90% of the cells retaining viability at 24 h after incubation (see Fig. 2). The observed low cytotoxicity could be attributed to several factors, especially contributed by their low-toxic emental consitituents. These results suggest that Ag_2S QDs are promising nanoparticles for bio-applications. We also verified the low toxicity of Ag_2S QDs through animal experiment. The mice injected with Ag_2S QDs (1062.5 μg/kg) did not show any abnormal symptoms, and were still alive after 2 weeks.

3.3. *Cell imaging*

The cellular uptake and intracellular localization of Ag_2S was detected using confocal laser scanning microscopy. MCF-7 cells were treated with 20 μL of QDs (0.425 mg/mL) for 2 and 4 h. Ag_2S NIR QDs were effectively internalized and exhibited a punctuated cytoplasmic distribution (see Fig. 3). QDs emitted fluorescence ranged from UV region to IR region were the research focus recently, and different kinds of QDs were applied for cell imaging and

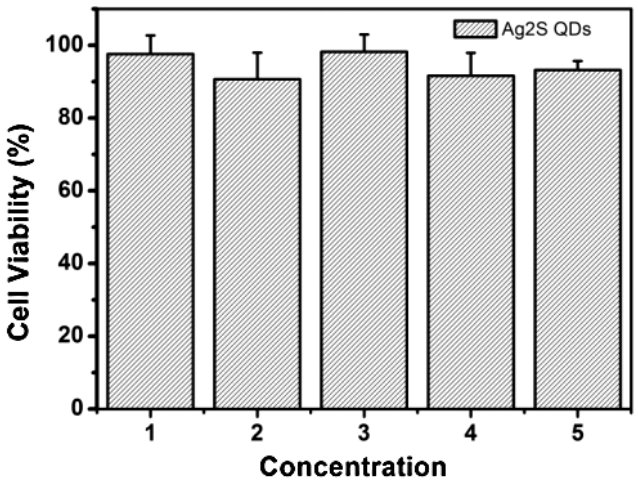

Fig. 2. Cell viability of the MCF-7 with different concentration of Ag_2S QDs.

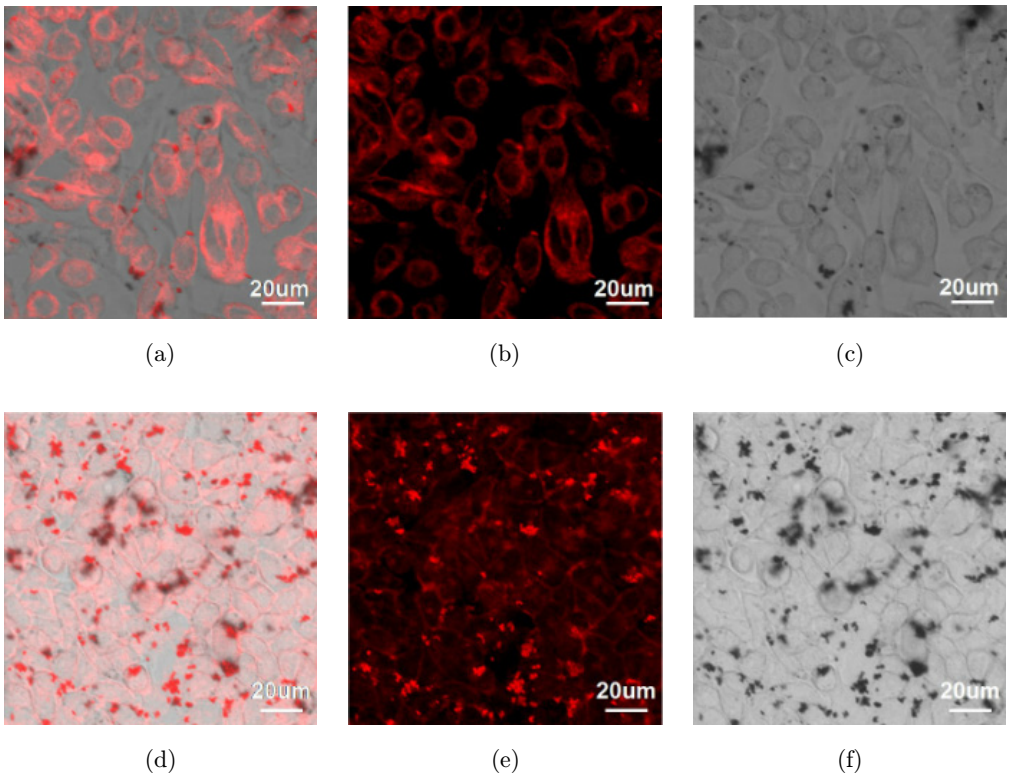

(a) (b) (c)

(d) (e) (f)

Fig. 3. Fluorescence microscopy images of MCF-7 cells stained with Ag_2S QDs at 2 h (a), (b) and (c) 4 h (d), (e) and (f). (b) and (e): fluorescence images; (c) and (f): bright field images; (a) and (d): merged images.

animal imaging successfully. However, the existed biotoxicity of the QDs prevented their further clinical application. Ag_2S QDs reported here aimed at seeking more bio-safe contrast agent for bioimaging. The red fluorescence QDs in our study displayed low biotoxicity and fast cell internalization, which provided a reference for the contrast agent research in future.

4. Conclusion

Colloidally stable, highly cytocompatible and highly luminescent aqueous Ag_2S NIR emitting QDs were successfully synthesized in water with a 3-MPA coating. The size and therefore the emission wavelength of these NIR QDs can be tuned between 800 and 830 nm. These particles possess significantly better quantum yield of 37.9% compared to reported values in the literature. In addition, these Ag_2S NIR QDs showed dramatically improved cytocompatibility in MCF-7 cell lines. Cell imaging studies demonstrated that Ag_2S NIR QDs are excellent fluorescence probe for bioimaging.

Acknowledgments

The authors are grateful to the Natural Science Foundation Committee of China (NSFC 81371684, 81000666, 81220108012, 61335007, 81171395 and 81328012), the Program for New Century Excellent Talents (NCET) at the University of the Ministry of Education of China and a project funded by the Priority Academic Program Development of Jiangsu Higher Education Institutions for their financial support.

References

1. W. C. W. Chan, S. Nie, "Quantum dot bioconjugates for ultrasensitive nonisotopic detection," *Science* **281**, 2016–2018 (1998).
2. M. Bruchez, M. Moronne, P. Gin, S. Weiss, A. P. Alivisatos, "Semiconductor nanocrystals as fluorescent biological labels," *Science* **281**, 2013–2016 (1998).
3. B. Dubertret, P. Skourides, D. J. Norris, V. Noireaux, A. H. Brivanlou, A. Libchaber, "*In vivo* imaging of quantum dots encapsulated in phospholipid micelles," *Science* **298**, 1759–1762 (2002).
4. X. Gao, Y. Cui, R. M. Levenson, L. W. K. Chung, S. Nie, "*In vivo* cancer targeting and imaging with

semiconductor quantum dots," *Nat. Biotechnol.* **22**, 969–976 (2004).
5. U. Resch-Genger, M. Grabolle, S. Cavaliere-Jaricot, R. Nitschke, T. Nann, "Quantum dots versus organic dyes as fluorescent labels," *Nat. Methods* **5**, 763–775 (2008).
6. E. I. AÌtinoglu, J. H. Adair, "Near infrared imaging with nanoparticles," *Wiley Interdiscip. Rev.: Nanomed. Nanobiotechnol.* **2**, 461–477 (2010).
7. P. Sharma, S. Brown, G. Walter, S. Santra, B. Moudgil, "Nanoparticles for bioimaging," *Adv. Colloid Interface Sci.* **123–126**, 471–485 (2006).
8. R. Aswathy, Y. Yoshida, T. Maekawa, D. Kumar, "Near-infrared quantum dots for deep tissue imaging," *Anal. Bioanal. Chem.* **397**, 1417–1435 (2010).
9. W. Jiang, A. Singhal, B. Y. S. Kim, J. Zheng, J. T. Rutka, C. Wang, W. C. W. Chan, "Deep tissue bioimaging using two-photon excited CdTe fluorescent quantum dots working within the biological window," *J. Assoc. Lab. Autom.* **13**, 6–12 (2008).
10. Y. T. Lim, S. Kim, A. Nakayama, N. E. Stott, M. G. Bawendi, J. V. Frangioni, "Selection of quantum dot wavelengths for biomedical assays and imaging," *Mol. Imaging* **2**, 50–64 (2003).
11. J. V. Frangioni, "*In vivo* near-infrared fluorescence imaging," *Curr. Opin. Chem. Biol.* **7**, 626–634 (2003).
12. S. Kim, Y. T. Lim, E. G. Soltesz, A. M. De Grand, J. Lee, A. Nakayama, J. A. Parker, R. G. Laurence, D. M. Dor, L. H. Cohn, M. G. Bawendi, J. V. Frangioni, "Near-infrared fluorescent type II quantum dots for sentinel lymph node mapping," *Nat. Biotechnol.* **22**, 93 (2004).
13. L. P. Balet, S. A. Ivanov, A. Piryatinski, M. Achermann, V. I. Klimov, "Inverted core/shell nanocrystals continuously tunable between type-I and type-II localization regimes," *Nano Lett.* **4**, 1485 (2004).
14. B. Blackman, D. Battaglia, X. G. Peng, "Coupled and decoupled dual quantum systems in one semiconductor nanocrystal," *Chem. Mater.* **20**, 4847 (2008).
15. P. M. Allen, M. G. Bawendi, "Ternary I-III-VI quantum dots luminescent in the red to near-infrared," *J. Am. Chem. Soc.* **130**, 9240 (2008).
16. L. Guo-Xi, G. Miao-Miao, Z. Jian-Rong, Z. Jun-Jie, "Preparation and bioapplication of high-quality, water-soluble, biocompatible, and near-infrared-emitting CdSeTe alloyed quantum dots," *Nanotechnology* **20**, 415103 (2009).
17. H. Y. Chen, S. S. Cui, Z. Z. Tu, J. Z. Ji, J. Zhang, Y. Q. Gu, "Characterization of CdHgTe/CdS QDs for near infrared fluorescence imaging of spinal column in a mouse model," *Photochem. Photobiol.* **87**, 72–81 (2011).
18. B. Blackman, D. Battaglia, X. Peng, "Coupled and decoupled dual quantum systems in one semiconductor nanocrystal," *Chem. Mater.* **20**, 4847–4853 (2008).
19. N. Y. Morgan, S. English, W. Chen, V. Chernomordik, A. Russo, P. D. Smith, A. Gandjbakhche, "Real time in vivo non-invasive optical imaging using near-infrared fluorescent quantum dots," *Acad. Radiol.* **12**, 313–323 (2005).
20. S. Kim, Y. T. Lim, E. G. Soltesz, A. M. De Grand, J. Lee, A. Nakayama, J. A. Parker, T. Mihaljevic, R. G. Laurence, D. M. Dor, L. H. Cohn, M. G. Bawendi, J. V. Frangioni, "Near-infrared fluorescent type II quantum dots for sentinel lymph node mapping," *Nat. Biotechnol.* **22**, 93–97 (2004).
21. H. Ding, K.-T. Yong, W.-C. Law, I. Roy, R. Hu, F. Wu, W. Zhao, K. Huang, F. Erogbogbo, E. J. Bergey, P. N. Prasad, "Non-invasive tumor detection in small animals using novel functional Pluronic nanomicelles conjugated with anti-mesothelin antibody," *Nanoscale* **3**, 1813–1822 (2011).
22. H. Kobayashi, M. Ogawa, R. Alford, P. L. Choyke, Y. Urano, "New strategies for fluorescent probe design in medical diagnostic imaging," *Chem. Rev.* **110**, 2620–2640 (2009).
23. A. M. Smith, H. Duan, A. M. Mohs, S. Nie, "Bioconjugated quantum dots for in vivo molecular and cellular imaging," *Adv. Drug Deliv. Rev.* **60**, 1226–1240 (2008).
24. R. G. Aswathy, Y. Yoshida, T. Maekawa, D. S. Kumar, "Near-infrared quantum dots for deep tissue imaging," *Anal. Bioanal. Chem.* **397**, 1417–1435 (2010).
25. A. J. Tavares, L. R. Chong, E. Petryayeva, W. R. Algar, U. J. Krull, "Quantum dots as contrast agents for in vivo tumor imaging: progress and issues," *Anal. Bioanal. Chem.* **399**, 2331–2342 (2011).
26. A. M. Smith, S. Nie, "Next-generation quantum dots" *Nat. Biotechnol.* **27**, 732–733 (2009).
27. P. Jiang, C.-N. Zhu, Z.-L. Zhang, Z.-Q. Tian, D.-W. Pang, "Water-soluble Ag(2)S quantum dots for near-infrared fluorescence imaging *in vivo*," *Biomaterials* **33**, 5130–5135 (2012).
28. I. Hocaoglu, M. N. Cizmeciyan, R. Erdem, C. Ozen, A. Kurt, A. Sennaroglu, H. Y. Acar, "Fabrication of vascular endothelial growth factor antibody bioconjugated ultrasmall near-infrared fluorescent Ag2S quantum dots for targeted cancer imaging *in vivo*," *J. Mater. Chem.* **22**, 14674–14681 (2012).
29. C. Wang, Y. Wang, L. Xu, D. Zhang, M. Liu, X. Li, H. Sun, Q. Lin, B. Yang, "Facile aqueous-phase synthesis of biocompatible and fluorescent Ag2S nanoclusters for bioimaging: Tunable photoluminescence from red to near infrared," *Small* **8**, 3137–3142 (2012).

30. H.-Y. Yang, Y.-W. Zhao, Z.-Y. Zhang, H.-M. Xiong, S.-N. Yu, "One-pot synthesis of water-dispersible Ag2S quantum dots with bright fluorescent emission in the second near-infrared window," *Nanotechnology* **24**, 055706 (2013).
31. I. Hocaoglu, M. N. Cizmeciyan, R. Erdem, C. Ozen, A. Kurt, A. Sennaroglu, H. Y. Acar, "Development of highly luminescent and cytocompatible near-IR-emitting aqueous Ag2S quantum dots," *J. Mater. Chem.* **22**, 14674 (2012).
32. M. Yarema, S. Pichler, M. Sytnyk, R. Seyrkammer, R. T. Lechner, G. Fritz-Popovski, D. Jarzab, K. Szendrei, R. Resel, O. Korovyanko, M. A. Loi, O. Paris, G. N. Hesser, W. Heiss, *ACS Nano* **5**, 3758–3765 (2011).
33. P. Jiang, Z.-Q. Tian, C.-N. Zhu, Z.-L. Zhang, D.-W. Pang, *Chem. Mater.* **24**, 3–5 (2011).
34. Y.-P. Gu, R. Cui, Z.-L. Zhang, Z.-X. Xie, D.-W. Pang, *J. Am. Chem. Soc.* **134**, 79–82 (2011).
35. Y. Zhang, Y. Zhang, G. Hong, W. He, K. Zhou, K. Yang, F. Li, G. Chen, Z. Liu, H. Dai, Q. Wang, *Biomaterials* **34**, 3639–3646 (2013).
36. G. Hong, J. T. Robinson, Y. Zhang, S. Diao, A. L. Antaris, Q. Wang, H. Dai, *Angew. Chem. Int. Ed.* **51**, 9818–9821 (2012).
37. Y. Zhang, G. Hong, Y. Zhang, G. Chen, F. Li, H. Dai, Q. Wang, *ACS Nano* **6**, 3695–3702 (2012).
38. S. Shen, Y. Zhang, L. Peng, Y. Du, Q. Wang, *Angew. Chem. Int. Ed.* **50**, 7115–7118 (2011).
39. Y. Du, B. Xu, T. Fu, M. Cai, F. Li, Y. Zhang, Q. Wang, *J. Am. Chem. Soc.* **132**, 1470–1471 (2010).